11. *Ibid.*, **24**, 1232 (1953).
12. Bird, R. B., W. E. Stewart, and E. N. Lightfoot, "Transport Phenomena," p. 14, Wiley, New York (1960).
13. Bizzell, G. D., and J. C. Slattery, *Chem. Eng. Sci.*, **17**, 777 (1962).
14. Blasius, H., *Z. Math. Phys.*, **58**, 225 (1910).
15. Clegg, P. L., in "The Rheology of Elastomers," Pergamon Press, New York (1958).
16. Collins, Morton, and W. R. Schowalter, *AIChE J.*, **9**, 98 (1963).
17. *Ibid.*, 804 (1963).
18. Drexler, L. H., M.Sc. thesis, Univ. Delaware, Newark (1967).
19. Gutfinger, Chaim, and Reuel Shinnar, *AIChE J.*, **10**, 631 (1964).
20. Hamel, G., *Jabresber. Dt. Mathematiker-Vereinigung*, **34**, (1916).
21. Hansen, A. G., "Similarity Analysis of Boundary Value Problems in Engineering," Prentice-Hall, Englewood Cliffs, N. J. (1964).
22. Hayasi, Nisiki, *J. Fluid Mech.*, 23, 293 (1965).
23. Hershey, H. C., and J. L. Zakin, *Ind. Eng. Chem. Fundamentals*, **6**, 381 (1967).
24. Jeffery, G. B., *Phil. Mag.*, **29**, 455 (1915).
25. Lee, S. Y., and W. F. Ames, *AIChE J.*, **12**, 700 (1966).
26. Metzner, A. B., *Ind. Eng. Chem.*, **50**, 1577 (1958).
27. ———, and Gianni Astarita, *AIChE J.*, 13, 550 (1967).
28. Metzner, A. B., J. L. White, and M. M. Denn, *ibid.*, **12**, 863 (1966).
29. ———, *Chem. Eng. Progr.*, **62**, 81 (1966).
30. Metzner, A. B., and J. L. White, *AIChE J.*, **11**, 989 (1965).
31. Metzner, A. B., W. T. Houghton, R. E. Hurd, and C. C. Wolfe, "Second Order Effects in Elasticity, Plasticity and Fluid Dynamics," p. 650, Pergamon Press, New York (1964).
32. Metzner, A. B., E. L. Carley, and I. K. Park, *Modern Plastics*, **37**, 133 (1960).
33. Millsaps, K. T., and Karl Pohlhausen, *J. Aero. Sci.*, 20, 187 (1953).
34. Mishra, S. P., and J. S. Roy, *Phys. Fluids*, 11, 2074 (1968).
35. Na, T. Y., and A. G. Hansen, *ASME Paper No. 67-WA/FE-2 (J. Basic Eng.)*.
36. Pearson, J. R. A., and C. J. S. Petrie, *Proc. 4th Intern. Rheol. Congr.*, **3**, 265 (1965).
37. Pohlhausen, Karl, *ZAMM*, **18**, 77 (1938).
38. Rosenhead, Louis, *Proc. Roy. Soc. London*, **175**, 436 (1940).
39. Savins, J. G., *Soc. Petrol. Eng. J.*, **4**, 203 (1964).
40. Schlichting, Hermann, "Boundary Layer Theory," 4th edit., McGraw-Hill, New York (1960).
41. Schowalter, W. R., *AIChE J.*, **6**, 24 (1960).
42. Sellars, J. R., *J. Appl. Phys.*, **26**, 489 (1955).
43. Seyer, F. A., and A. B. Metzner, *Can. J. Chem. Eng.*, **45**, 121 (1967).
44. Slattery, J. C., *AIChE J.*, **14**, 516 (1968).
45. Smith, D. K., Ph.D. dissertation, North Carolina State Univ., Raleigh (1965).
46. Spencer, R. S., and J. E. Dillon, *J. Colloid Sci.*, **4**, 241 (1949).
47. Tordella, J. P., *J. Appl. Polymer Sci.*, **7**, 215 (1963).
48. ———, *Rheol. Acta*, **1**, 216 (1958).
49. ———, *Trans. Soc. Rheo.*, **1**, 203 (1957).
50. ———, *J. Appl. Phys.*, **27**, 454 (1956).
51. Uebler, E. A., Ph.D. dissertation, Univ. Delaware, Newark (1966).
52. Weissenberg, Karl, "Proceedings of the First International Rheology Congress," pp. 1, 29, Scheveningen (1949).
53. White, J. L., *J. Appl. Polymer Sci.*, **8**, 2339 (1964).
54. ———, and N. J. Tokita, *ibid.*, **10**, 1011 (1966).
55. White, J. L., and A. B. Metzner, *AIChE J.*, **11**, 324 (1965).
56. Williams, J. C. III, *AIAA J.*, **1**, 186 (1963).
57. ———, *USCEC Rept. 83-213* (June 1962).
58. Yuan, S. W., *J. Appl. Phys.*, **27**, 267 (1956).

Manuscript received October 8, 1968; revision received July 28, 1969; paper accepted July 31, 1969.

Polymerization in Expanding Catalyst Particles

W. R. SCHMEAL and J. R. STREET[a]

Shell Development Company, Emeryville, California

Four models are presented to describe polymerization in expanding catalyst particles. The globules are presumed to be expanding with accumulating polymer, and catalytic reaction sites are dispersed throughout the polymer matrix which is forming about them. Monomer must diffuse through the polymer to polymerize at the catalyst sites.

The Thiele modulus (α), $R\sqrt{kl/D}$, is a ratio of characteristic diffusion time to reaction time which is a measure of the importance of diffusion relative to reaction. Polymerization rates are predicted by the models which are generally dependent on the controlling mechanism. Broad molecular weight distributions are predicted for cases of diffusion control (large α) for those models in which catalyst sites are not equally accessible to monomer.

Polymerization rates decline toward an asymptotic final value as the particles expand in diffusion-controlled cases. Most of the decline which would be readily observable in a laboratory experiment would have occurred by the time the particle radii had increased to about three times their original value.

Solid polymerization catalysts fluidized in a material that does not dissolve the polymer expand with accumulating polymer during reaction. These particles may grow more than 10,000-fold in volume during polymerization. In fact, since catalysts are generally much more expensive per unit weight than the polymers they produce, a considerable increase in size during polymerization is usually a prerequisite for the associated process to have commercial value. Otherwise, the catalyst must be recovered.

[a]Present address, Shell Chemical Company, Deer Park, Texas.

The polymerization of α-olefins via a Ziegler catalyst is an example of the above type (*2, 3, 6, 7, 10, 11, 14, 16, 17*). Presumably others will fall into this class, such as the generally insoluble polymers like polyphenylene (*13*).

We will consider four physical models for polymerization featuring high yield. In each, monomer diffuses into the catalyst particle and combines with a polymer chain attached to a reaction site. The particle is assumed to be polymeric because the catalyst is quickly diluted in accumulating polymer. The addition is presumed to occur at the site

$$M + L_i \longrightarrow L_{i+1}$$

L_i is a polymer chain of i units of the monomer M, and it is alive and attached to a site. An empty site is denoted by L_0. More complex kinetics will be considered in a later paper; physical mechanisms are to be emphasized here.

In the expansion models sites are considered to move outward as they are engulfed and diluted with the polymer they are producing. Sites are assigned a concentration l which may be a function of radial position and time.

There are a variety of ways in which reaction sites may be transported during polymerization (for example, as parts of moving catalyst chunks). Perhaps none of the actual mechanisms that exist corresponds exactly to any of our proposed models. It is hypothesized, however, that the models which are presented are limiting cases for numerous actual mechanisms.

Various morphological possibilities are covered as well. Particle macrostructure may develop for some reason, resulting in a porous globule. Our models would then describe an individual subparticle, provided its characteristic diffusion time $R^2/\pi^2 D$ were greater than that for the entire particle. R is the pertinent radius before expansion and D is the appropriate diffusivity.

Extremely simple chemical kinetics are considered and the particles are assumed to be spherical. Mass transfer in the continuous fluid phase is assumed not to limit the reaction and monomer is thus assumed to be at thermodynamic equilibrium between the fluid and the (polymeric) particles. Particle expansion effects will be considered here and polymerization rates and molecular weight distributions will be calculated for the various models. We will consider some other effects in subsequent studies.

PHYSICAL MODELS

Frequent reference will be made to the base model because of its simplicity. For this model, it is assumed that a nonexpanding polymeric particle has sites distributed evenly throughout it with concentration l. This model may be realistic in some cases because radius increases only as the cube root of volume increases and the relative growth of a particle (dr/rdt) slows after the initial stages of polymerization. The model, because of its simplicity, serves as a convenient base case for investigation of the effects of complicating phenomena.

The solid core model is another good reference model because it is elementary. Here, polymer is assumed to accumulate about a catalyst sphere, the surface of which supports the polymerization. Monomer diffuses through the growing polymeric coat. Both Begley (*2*) and Seinfeld (*16*) have chosen this model for their studies of propylene polymerization. They have considered cases of more complicated kinetics than have been introduced here.

These models provide a base for the study of the expansion models. It is desirable to provide for a generalized mechanism of site transport in the growing particles. To do this, two limiting case models are considered: one in which sites move infinitely slowly, the polymeric core model; and one in which sites move at a maximum velocity consistent with the conservation of mass, the flow model. In the first, the sites are distributed evenly throughout a stationary inner polymeric sphere. Site concentration is a function of radius and time in the second model and the base model is used as an initial condition. Numerical solutions are presented for the moving boundary problems presented by the flow model and analytical solutions are derived for the polymeric core model.

REACTION RATES

It is of interest to observe how the various physical and chemical parameters affect the polymerization rate, according to the predictions of the models. We shall also emphasize the behavior of the specific polymerization rate versus time, because both constant (*3, 7, 14*) and declining (*6, 11*) rates are noted for α-olefin polymerizations that are presumably analogous.

The conservation of mass may be expressed in dimensionless form for the base model as

$$\frac{1}{\eta^2}\frac{\partial}{\partial \eta}\left(\eta^2 \frac{\partial c}{\partial \eta}\right) - \alpha^2 c = \frac{\partial c}{\partial \tau} \tag{1}$$

Boundary conditions are

$$\frac{\partial c}{\partial \eta} = 0 \qquad \eta = 0$$

$$c = c_s \qquad \eta = 1$$

A distribution coefficient K_D, a ratio of volumetric molar concentrations in polymer and solvent, is included in the definition of the dimensionless concentration of monomer in the fluid medium c_s.

We shall assume throughout that the characteristic time of the processes taking place within the particle is shorter than the residence time of the reactor, so that the accumulation term may be discarded in Equation (1). Investigation of Equation (1) using LaPlace transforms shows that the predominant decay term is $\exp[-(\alpha^2 + \pi^2)\tau]$. Reassignment of dimensions yields the following expressions for characteristic time T:*

$$T = \frac{1}{kl} \quad \text{for} \quad \alpha \gg 1$$

$$T = \frac{R^2}{\pi^2 D} \quad \text{for} \quad \alpha \ll 1$$

We shall show later that in general large α means diffusion control and small α indicates reaction control.

The solution for Equation (1) without its capacity term is

$$c = c_s \frac{\sinh \alpha\eta}{\eta \sinh \alpha} \tag{2}$$

Thus the dimensionless flux of monomer at the particle surface is

$$\left(\frac{\partial c}{\partial \eta}\right)_{\eta=1} = c_s(\alpha \coth \alpha - 1) \tag{3}$$

From this, it may be seen that the specific reaction rate, or volumetric rate of disappearance of monomer divided by monomer concentration in the fluid, is proportional to

$$f(\alpha) = \alpha \coth \alpha - 1 \tag{4}$$

This specific rate is constant versus time and a function of the physical parameters.

*Characteristic time T means the process decays like $\exp(-t/T)$.

The limits of $f(\alpha)$ for large and small α are of interest. It is apparent that

$$\lim_{\alpha\to\infty} f(\alpha) = \alpha \tag{5}$$

$f(\alpha)$ has a second-order zero at the origin. Note, however, that

$$\lim_{\alpha\to 0} \frac{f(\alpha)}{\alpha^2} = \lim_{\alpha\to 0} \frac{1}{\alpha^2}\left[\frac{\alpha\left(1+\frac{\alpha^2}{2}+\cdots\right)}{\left(\alpha+\frac{\alpha^3}{6}+\cdots\right)} - 1\right]$$

$$= \lim_{\alpha\to 0} \frac{1}{\alpha^2} \frac{\left(\frac{\alpha^2}{3}+\cdots\right)}{\left(1+\frac{\alpha^2}{6}+\cdots\right)}$$

Using the Taylor expression

$$\frac{1}{1-x} = \sum_{n=0}^{\infty} x^n$$

we find that

$$\lim_{\alpha\to 0} \frac{f(\alpha)}{\alpha^2} = \frac{1}{\alpha^2}\left(\frac{\alpha^2}{3}+\cdots\right)\left(1-\frac{\alpha^2}{6}+\cdots\right) = \frac{1}{3}$$

For small α then

$$f(\alpha) \approx \frac{\alpha^2}{3} \tag{6}$$

Reassigning dimensions, the specific reaction rate defined above is

$$k^* = \frac{D}{R^2} G f(\alpha) \tag{7}$$

For large α

$$k^* = \frac{3V_p K_D}{R}\sqrt{Dkl} \tag{8}$$

and for small α

$$k^* = V_p K_D kl \tag{9}$$

For small α, the process is reaction controlled and the monomer has complete and unhindered access to every reaction site. The specific polymerization rate is proportional to the number of sites per unit volume of solution and the activity of these sites. For large α the process is weakly dependent (to the square root) on site activity, number of sites, and monomer diffusivity in the polymeric medium. In both extremes, specific rate is proportional to monomer solubility in the polymer.

RATES FOR THE SOLID CORE MODEL

In the solid core model, reaction occurs at the surface of an inner core and monomer diffuses through its growing polymeric coat. The pertinent conservation equation for the outer coat is, in dimensionless form

$$\frac{1}{\eta^2}\frac{\partial}{\partial\eta}\left(\eta^2\frac{\partial c}{\partial\eta}\right) = 0 \tag{10}$$

The accumulation term has been ignored. The boundary conditions are

$$\frac{\partial c}{\partial\eta} = \frac{\alpha^2 c}{3} \qquad \eta = 1$$
$$c = c_s \qquad \eta = \eta_s \tag{11}$$

A factor of 3 is introduced to make this development correspond to that for the base model and the polymeric core model. η_s is the dimensionless radius of the entire sphere, which increases in proportion to the generation of polymer, or the flux of monomer at the surface of the sphere (since the accumulation term has been ignored). That is

$$\eta_s^2 \frac{d\eta_s}{d\tau} = \frac{\gamma}{3}\frac{dp}{d\tau} = \gamma\left(\frac{\partial c}{\partial\eta}\right)_{\eta=1} \tag{12}$$

Equations (10) and (11) may be solved and the monomer flux calculated:

$$\left(\frac{\partial c}{\partial\eta}\right)_{\eta=1} = \frac{\alpha^2 c_s}{3+\alpha^2\left(\frac{\eta_s-1}{\eta_s}\right)} \tag{13}$$

Dimensions may be reassigned so that the specific rate constant may be calculated:

$$k^* = \frac{D}{R^2} G \frac{\alpha^2}{3+\alpha^2\left(\frac{\eta_s-1}{\eta_s}\right)} \tag{14}$$

Here V_p refers to the volume of catalyst excluding the polymer per unit reactor volume and R is the solid core radius.

Note that for large α

$$k^* \longrightarrow \frac{D}{R^2} G \frac{\eta_s}{\eta_s - 1} \qquad \eta_s > 1 \tag{15}$$

and for small α

$$k^* \longrightarrow \frac{D}{3R^2} G\alpha^2, \tag{16}$$

Thus large α implies complete diffusion control with specific rate constant declining to an asymptotic value as the particle grows:

$$k^* \longrightarrow \frac{3D V_p K_D}{R^2} \tag{17}$$

Small α indicates reaction control and a specific rate constant independent of particle size:

$$k^* \longrightarrow V_p K_D k \tag{18}$$

For the last case of reaction control the solid core model and the base model predict results which are indistinguishable because the important processes are not transport limited.

The results for the solid core model for the case of diffusion control given in Equation (17) show complete independence of the specific reaction rate upon the actual chemical rate constant. Thus apparent catalyst activity is a function only of monomer permeability and catalyst size. The predicted rate decline is worthy of closer investigation.

Let us find the relationships among the specific rate constant, the sizes of the growing spheres, and the amount of polymer produced. The solution to the left equality in Equation (12) is

$$\eta_s^3 = 1 + \gamma p \tag{19}$$

γp is the volumetric ratio of polymer to solid catalyst. Equation (19) merely states that the relative particle radius is proportional to the cube root of relative volume.

The relation between particle radius and specific reaction rate is given by Equation (14), which may be

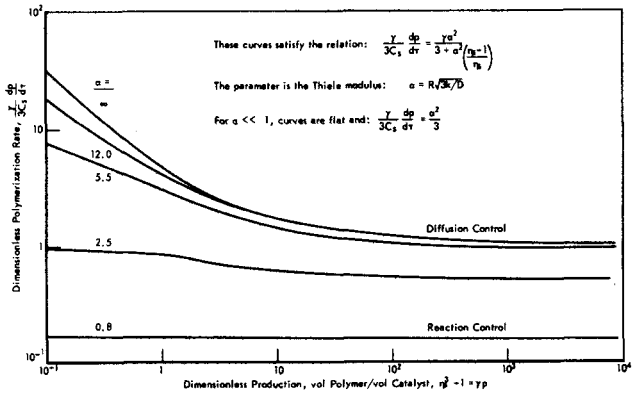

Fig. 1. Dimensionless polymerization rate versus dimensionless polymer production predicted by the solid core model.

rearranged:

$$\frac{1}{\eta_s} = 1 + \frac{3}{\alpha^2} - \frac{GD}{k^* R^2} \tag{20}$$

Equations (19) and (20) give a relationship between specific reaction rate and polymer production:

$$k^* = \frac{\dfrac{3V_p K_D D}{R^2}}{1 + \dfrac{3}{\alpha^2} - \dfrac{1}{\sqrt[3]{1+\gamma p}}} = \frac{\dfrac{3V_p K_D D}{R^2}}{1 + \dfrac{3}{\alpha^2} - \dfrac{1}{\eta_s}} \tag{21}$$

Thus k^* begins at $V_p K_D k$ at time zero, indicating that there is no diffusive resistance [see Equation (18)]. As polymer production γp increases, k^* declines to the asymptote given by Equation (17). Typical curves for specific reaction rate versus polymer production in dimensionless form are shown in Figure 1 for various Thiele moduli α. Equations (12) and (13) are used to construct this figure.

REACTION RATES FOR THE EXPANSION MODELS

In the expansion models reaction occurs at active sites which are embedded in polymer and which are moving radially outward. Therefore, as stated previously, we consider two limiting cases for the expansion models—the polymeric core model, in which sites move infinitely slowly, and the flow model, in which sites move with the velocity of the polymer surrounding them. In both of these cases reaction rate expressions are similar to those derived for the solid core model. In fact, the solid core model and the polymeric core model predict identical rates. It will be shown later that the molecular weight distributions predicted by these models are quite different, however.

The equations of conservation of mass for the polymeric core model are, in dimensionless form

$$\frac{1}{\eta^2}\frac{\partial}{\partial \eta}\left(\eta^2 \frac{\partial c}{\partial \eta}\right) - \alpha^2 c = 0 \quad \text{inner sphere} \tag{22}$$

$$\frac{1}{\eta^2}\frac{\partial}{\partial \eta}\left(\eta^2 \frac{\partial c}{\partial \eta}\right) = 0 \quad \text{outer sphere} \tag{23}$$

with boundary conditions

$$\frac{\partial c}{\partial \eta} = 0 \qquad \eta = 0$$

$$c, \frac{\partial c}{\partial \eta} \text{ continuous} \qquad \eta = 1$$

$$c = c_s \qquad \eta = \eta_s$$

The development of the rate expressions for the polymeric core model is the same as that for the solid core model, except that the definitions of the rate constants k and thus the Thiele modulus α are different. In the latter case the rate constant represents a constant for surface reaction and in the former case, the first order constant k represents the constant for a volumetric rate as in the base model.

The solutions to Equation (22) for $c(\eta)$ and its first derivative are analogous to Equations (2) and (3):

$$c(\eta) = c(1)\frac{\sinh \alpha\eta}{\eta \sinh \alpha} \tag{24}$$

and

$$\frac{\partial c}{\partial \eta} = c(1)(\alpha \coth \alpha - 1) \quad \text{for } \eta = 1 \tag{25}$$

Thus Equations (22) and (23) may be replaced by the equations for the solid core model, Equations (10) and (11), except that the latter must be modified to

$$\frac{\partial c}{\partial \eta} = (\alpha \coth \alpha - 1)c \qquad \eta = 1$$
$$c = c_S \qquad \eta = \eta_s \tag{11a}$$

The development for polymerization rate for the polymeric core model proceeds as in Equations (12) to (21), except that $\alpha^2/3$ must everywhere be replaced by $\alpha \coth \alpha - 1$ or $f(\alpha)$ [see Equation (4)].

The values of $f(\alpha)$ in the limits of large and small (positive) α are given in Equations (5) and (6). It follows that the results derived for the solid core model for these limits, Equations (15), (17), and (18), also apply in the case of the polymeric core model. Figure 1 also applies except that $\alpha^2/3$ becomes $f(\alpha)$ as noted above.

RATES FOR THE FLOW MODEL

Reaction sites are free to move or flow outward with the polymer according to the limiting case of the expansion models, which we call the flow model. Continuity equations must be constructed in this model not only for monomer, but for polymer and catalyst sites. These are

$$D\frac{1}{r^2}\frac{\partial}{\partial r}\left(r^2\frac{\partial M}{\partial r}\right) - klM = \frac{\partial M}{\partial t} \quad \text{monomer} \tag{26}$$

$$\rho\frac{1}{r^2}\frac{\partial}{\partial r}(ur^2) - klM = 0 \quad \text{polymer} \tag{27}$$

$$-\frac{1}{r^2}\frac{\partial}{\partial r}(ulr^2) = \frac{\partial l}{\partial t} \quad \text{catalyst sites} \tag{28}$$

Note that the incompressible polymer of molar density ρ (moles of monomer/volume) is convected with velocity u and is formed via reaction. The sites are convected also with velocity u and accumulate locally at a rate of $\partial l/\partial t$.

In dimensionless form, these equations are

$$\frac{1}{\eta^2}\frac{\partial}{\partial \eta}\left(\eta^2\frac{\partial c}{\partial \eta}\right) - \alpha^2\theta c = 0 \tag{29}$$

$$\frac{1}{\eta^2}\frac{\partial}{\partial \eta}(\eta^2 v) - \gamma\alpha^2\theta c = 0 \tag{30}$$

$$-\frac{1}{\eta^2}\frac{\partial}{\partial \eta}(\eta^2\theta v) = \frac{\partial \theta}{\partial \tau} \tag{31}$$

Again the accumulation term $\partial c/\partial\tau$ has been neglected in

Equation (29). The boundary conditions are

$$\begin{aligned} \frac{\partial c}{\partial \eta} = \frac{\partial \theta}{\partial \eta} = v = 0 \quad & \eta = 0 \\ c = c_S \quad & \eta = \eta_S \\ \theta = c = c_S = 1 \quad & \tau = 0 \end{aligned} \tag{32}$$

A condition is needed to describe the variation of monomer concentration in solution c_S. For example, for a batch

$$-\frac{dc_S}{d\tau} = G\left(\eta^2 \frac{\partial c}{\partial \eta}\right)_{\eta=\eta_s} \tag{33}$$

For a particle in a continuous stirred-tank reactor at steady state

$$\frac{dc_S}{d\tau} = 0$$

Other expressions for c_S may be defined corresponding to other reactor systems.

Equations (29) to (31) may be simplified. Equations (29) and (30) imply

$$v = \gamma \frac{\partial c}{\partial \eta} \tag{34}$$

This and Equation (31) yield

$$\frac{\partial \theta}{\partial \tau} + v \frac{\partial \theta}{\partial \eta} = -\gamma \alpha^2 \theta^2 c \tag{35}$$

We will replace the set of Equations (29) to (31) by the equivalent set, Equations (29), (34), and (35). This set will be solved numerically for cases of diffusion control $\alpha >> 1$.

Define two independent variables, μ and s, which are the characteristics of Equation (35).

$$\left(\frac{\partial \tau}{\partial s}\right)_\mu = 1 \qquad \left(\frac{\partial \eta}{\partial s}\right)_\mu = v \tag{36}$$

By the chain rule of partial differentiation, θ is determined as a function of s by an ordinary differential equation along curves of constant μ:

$$\left(\frac{\partial \theta}{\partial s}\right)_\mu = \frac{d\theta}{ds} = -\gamma \alpha^2 \theta^2 c \tag{37}$$

It also follows that

$$\left(\frac{\partial \theta}{\partial \tau}\right)_\mu = -\gamma \alpha^2 \theta^2 c \tag{38}$$

The curves of constant μ are the characteristic curves of the first-order partial differential equation (35) and sketches of them in the (η, τ) plane are shown in Figure 2. By Equation (36), the rate of change of radius with time along one of these curves is v, the catalyst site velocity. Thus the curves are what are known in fluid mechanics as particle paths (*1*). Therefore the sites move outward within the particle along trajectories which are the characteristics of Equation (35). The curve which intersects $\eta = 1$ at time zero ($\tau = 0$) represents the surface of the globule.

We have solved the set of Equations (29), (34), and (35) by integrating Equation (38) along a set of characteristics using the numerical procedure of Runge-Kutta (*9*). The particular characteristic curves are chosen by dividing the (radial) η axis into increments at time $\tau = 0$. The slope of each characteristic curve in the (η, τ) plane is $v(\eta, \tau)$, and is given by Equation (34). Each time the monomer concentration c is needed, Equation (29) must be solved.

We solved Equation (29) exactly (locally) in the intervals $\Delta\eta$ adjacent to each characteristic using a constant value of θ evaluated at the characteristic. The solutions were then expanded in Taylor series about their generating characteristic and all terms in $\eta - \eta_i$ of order greater than 2 were discarded. We noted that the error for this truncation was of the order of

$$[\alpha \sqrt{\theta}\,(\eta - \eta_i)]^4$$

This provided the criterion for choosing the sizes of the intervals $\Delta\eta$ between characteristic curves. We chose the condition that initially

$$\Delta\eta < 0.4\,\alpha \sqrt{\theta}$$

unless $\alpha < 10$, in which case

$$\Delta\eta < 4 \sqrt{\theta}$$

Whenever the curves grew apart as τ increased, so that $\Delta\eta$ exceeded $\alpha\sqrt{\theta}/2$, the increment was halved by the construction of a new characteristic curve between the two diverging ones.

Our results showed a similarity between this flow model and the polymeric core model but with a somewhat greater rate exhibited by the former. A comparison of rate versus production curves for the two models is shown in Figure 3 for a diffusion-controlled case of $\alpha = 48$. One would assume that an expansion model involving sites which were hindered somehow as they moved outward would feature a rate curve which fell between those limiting case curves shown in the figure. Note that a declining rate is predicted that levels out above a production of about 10 to 20 vol. of polymer per volume of catalyst. This is a two- to threefold increase in particle radius.

It is of interest to observe the paths of the reaction sites during polymerization as predicted by the flow model. Figure 4 shows these characteristic curves for the diffusion-controlled case $\alpha = 48$. Note that it is the sites in an

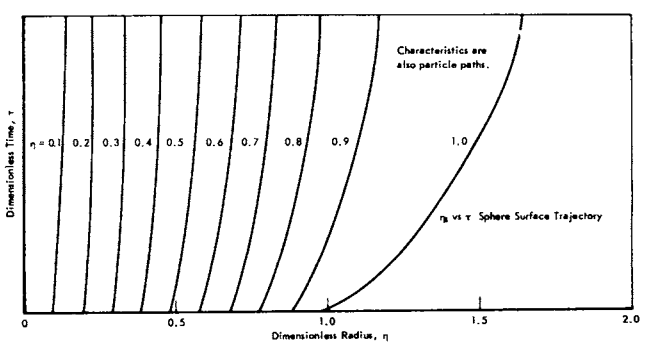

Fig. 2. Sketch of the characteristics or lines of constant μ of the partial differential Equation (35) for the flow model.

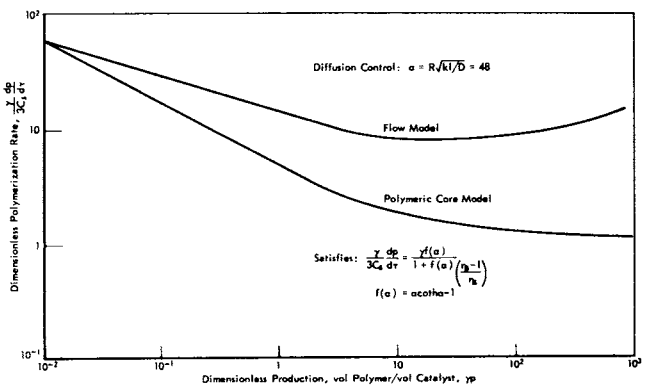

Fig. 3. Rate versus production predicted by the limiting case expansion models, the polymeric core model, and the flow model for a case of diffusion control.

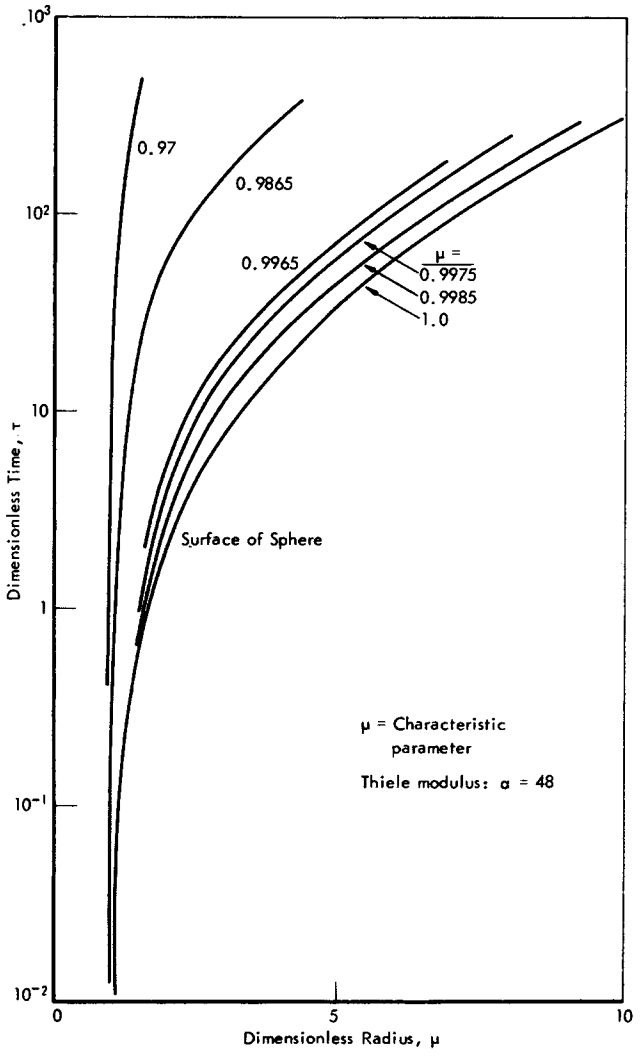

Fig. 4. Characteristics or paths of catalyst sites as predicted by the flow model for diffusion-controlled reaction.

outer shell of the catalyst which support the reaction. A site which resides initially at a radius, $\eta = 0.9$, will not be pulled outward appreciably, indicating that there is not much reaction occurring on the site and that it is starved of monomer.

In the reaction-controlled cases of small α, diffusion is no restriction and all the sites are equally accessible to monomer. All sites move outward because they are supporting reaction and polymer is being produced about them. The size of the globule does not affect the total polymerization rate, and sites should be equally distributed throughout the polymer globule.

MOLECULAR WEIGHT DISTRIBUTIONS

Broad molecular weight distributions are predicted for cases of diffusion control (large α) for those models in which sites are distributed throughout polymer, the base model, polymeric core model, and flow model, in particular. The solid core model, on the other hand, would predict a narrow distribution because, although the sites are buried in polymer, they are equally accessible.

We shall describe molecular weight distributions by their moments and certain ratios of these. Let l_i be the number of sites per unit volume to which polymer chains of length i are attached. Thus l_0 represents the concentration of empty sites. Define the number average and weight average molecular weights M_N and M_W (4):

$$M_N = m \frac{\sum_{i=0}^{\infty} i l_i}{\sum_{i=0}^{\infty} l_i}$$

$$M_W = m \frac{\sum_{i=0}^{\infty} i^2 l_i}{\sum_{i=0}^{\infty} i l_i} \tag{39}$$

We shall define the ratio of these as the Q value

$$Q = \frac{M_W}{M_N} = \frac{\sum_{i=0}^{\infty} l_i \sum_{i=0}^{\infty} i^2 l_i}{\left(\sum_{i=0}^{\infty} i l_i\right)^2} \tag{40}$$

Note that this expression is merely a ratio of moments.

The Q value can be a measure of the broadness of a distribution, although bimodal as well as polymodal distributions can have high Q values. A spikelike distribution has the minimum Q value of any distribution, $Q = 1$.

We shall use, in the following developments, a dimensionless site concentration θ_i

$$\theta_i = l_i / l_A$$

The θ_i may be substituted directly into Equation (40) for the l_i since the reference concentration cancels out.

STATIONARY SITE MODELS

We shall develop an expression for the Q value of the molecular weight distribution valid for any model in which the sites do not move such as the base model, the polymeric core model, or solid core model. We will use the very simple kinetic scheme described earlier, although this is not a restriction to the use of the methods.

The conservation of mass in dimensionless form for the chains of length i (units of monomer) applied locally is

$$\frac{d\theta_i}{d\tau} = (\beta\alpha^2) c\,(\theta_{i-1} - \theta_i) \quad i = 1, 2, \cdots \tag{41}$$

$$\frac{d\theta_0}{d\tau} = -(\beta\alpha^2) c\theta_0$$

Define the n^{th} moment of the distribution θ_i by λ_n

$$\lambda_n = \sum_{i=0}^{\infty} i^n \theta_i \tag{42}$$

The set of Equations (41) may be operated upon to yield equations for the moments Thus

$$\lambda_0 = \sum_{0}^{\infty} \theta_i = \theta \tag{43}$$

$$\frac{d\lambda_1}{d\tau} = \beta\alpha^2 c\theta$$

$$\frac{d\lambda_2}{d\tau} = \beta\alpha^2 c\,(2\lambda_1 + \theta)$$

These are local values and they must be integrated over the sphere to yield the moments λ_n^* appropriate to the en-

tire particle. Note that the total concentration of sites on the sphere is

$$\theta_i^* = \frac{4\pi \int_0^{\eta_s} \theta_i \eta^2 d\eta}{\frac{4}{3}\pi \eta_S^3} \tag{44}$$

Direct operations upon this give expressions for the particle moments

$$\lambda_n^* = \frac{3}{\eta_s^3} \int_0^{\eta_S} \eta^2 \lambda_n d\eta \tag{45}$$

It follows that the particle Q value is

$$Q^* = \frac{\lambda_2^* \lambda_0^*}{(\lambda_1^*)^2} = \frac{\int_0^{\eta_S} \eta^2 \lambda_2 d\eta \int_0^{\eta_S} \eta^2 \lambda_0 d\eta}{\left[\int_0^{\eta_S} \eta^2 \lambda_1 d\eta\right]^2} \tag{46}$$

We shall demonstrate a method of solving the differential equations (43) and evaluating Q^* by Equation (46) which applies to situations in which the sites are not necessarily distributed evenly throughout the particle. Let the radial distribution of sites be described by $\theta(\eta)$. Then the conservation of mass for monomer in dimensionless form is

$$\frac{1}{\eta^2}\frac{\partial}{\partial \eta}\left(\eta^2 \frac{\partial c}{\partial \eta}\right) - \alpha^2 \theta(\eta)\, c = 0 \quad 0 \le \eta \le 1 \tag{47}$$

This is analogous to Equations (1) and (22) and the accumulation term has been ignored.

The boundary conditions are

$$\frac{\partial c}{\partial \eta} = 0 \qquad \text{at } \eta = 0$$
$$c = c^*(\tau) \quad \text{at } \eta = 1 \tag{48}$$

There may or may not be a polymer coat existing outside the defined sphere, that is, for $\eta > 1$. The time-dependent monomer concentration $c^*(\tau)$ contains all the information about the processes outside the sphere containing the sites. The solution to this problem is

$$c(\eta, \tau) = c^*(\tau)\phi(\eta) \tag{49}$$

where $\phi(\eta)$ satisfies Equation (47) and the boundary conditions

$$\phi'(0) = 0 \quad \phi(1) = 1$$

The local zero moment is, of course

$$\lambda_0 = \theta(\eta)$$

The local first moment is described by Equation (43) and may be found by a direct integration:

$$\lambda_1(\eta, \tau) = \beta\alpha^2 \theta\phi \int_0^{\tau} c^*(\tau')\, d\tau' \tag{50}$$

A new dependent variable p is suggested by Equation (47) to evaluate the above integral. This may be related to time τ by Equation (12):

$$\frac{dp}{d\tau} = 3\left(\frac{\partial c}{\partial \eta}\right)_{\eta=1} \tag{12}$$

p is the dimensionless amount of polymer formed and will be substituted for τ in the following development. It follows from Equation (47) that

$$\left(\frac{\partial c}{\partial \eta}\right)_{\eta=1} = \alpha^2 \int_0^1 c\theta(\eta)\, \eta^2 d\eta \tag{51}$$

Thus

$$\frac{dp}{d\tau} = 3\alpha^2 c^*(\tau) \int_0^1 \theta(\eta)\phi(\eta)\eta^2 d\eta \tag{52}$$

A direct integration gives

$$p = 3\alpha^2 \int_0^1 \theta\phi\eta^2 d\eta \int_0^{\tau} c^* d\tau \tag{53}$$

This may be substituted into Equation (50):

$$\lambda_1 = \frac{\beta\theta\phi p}{3\int_0^1 \theta\phi\eta^2 d\eta} \tag{54}$$

Integration according to Equation (45) gives the first moment over the particle

$$\lambda_1^* = \beta p \tag{55}$$

This expression might have been deduced by noting that the number average molecular weight is the weight of polymer divided by the number of chains. A direct integration for the second moment according to Equation (43) gives

$$\lambda_2 = \lambda_1 + \frac{2\beta^2\alpha^2\theta\phi^2 \int_0^{\tau} pc^* d\tau'}{3G\int_0^1 \theta\phi\eta^2 d\eta} \tag{56}$$

The integral in the numerator may be simplified by using Equation (52). This may be rearranged to give

$$c^* = \frac{dp/d\tau}{3\alpha^2 \int_0^1 \theta\phi\eta^2 d\eta} \tag{57}$$

Thus

$$\int_0^{\tau} pc^* d\tau' = \frac{\int_0^{\tau} p \frac{dp}{d\tau'} d\tau'}{3\alpha^2 \int_0^1 \phi\theta\eta^2 d\eta} = \frac{p^2}{6\alpha^2 \int_0^1 \phi\theta\eta^2 d\eta} \tag{58}$$

There the local second moment is

$$\lambda_2 = \lambda_1 + \frac{\beta^2\theta\phi^2 p^2}{9\left[\int_0^1 \phi\theta\eta^2 d\eta\right]^2} \tag{59}$$

The second moment over the entire globule is given by an integration like Equation (45):

$$\lambda_2^* = \lambda_1^* + \frac{\beta^2 p^2 \int_0^1 \theta\phi^2\eta^2 d\eta}{3\left[\int_0^1 \theta\phi\eta^2 d\eta\right]^2} \tag{60}$$

Thus the Q value for the sphere is

$$Q^* = \frac{3\int_0^1 \theta\eta^2 d\eta}{\beta p} + \frac{\int_0^1 \theta\phi^2\eta^2 d\eta \int_0^1 \theta\eta^2 d\eta}{\left[\int_0^1 \theta\eta^2 d\eta\right]^2} \tag{61}$$

Note that the second term is independent of time or polymer accumulation and the first decays away in time. Furthermore, we have not specified what type of reactor is used since this information is contained in $c^*(\tau)$. Thus the results apply equally to a particle in a batch reactor, continuous stirred tank, or semicontinuous batch. The results also apply to a particle that has been in several reactors provided the total time spent adjusting to steady monomer profiles has been small.

Let us consider several specific examples. For either the base model or the polymeric core model, the site concentration is constant over the sphere $\theta(\eta) = 1$ and the monomer profile is given by Equation (2);

$$\phi(\eta) = \frac{\sinh \alpha\eta}{\eta \sinh \alpha} \tag{62}$$

Thus, the integrals in Equation (61) are

$$\int_0^1 \theta\eta^2 d\eta = \frac{1}{3}$$

$$\int_0^1 \theta\phi\,\eta^2 d\eta = \frac{\alpha \cosh \alpha - \sinh \alpha}{\alpha^2 \sinh \alpha} \tag{63}$$

$$\int_0^1 \theta\phi^2 \eta^2 d\eta = \frac{\sinh 2\alpha - 2\alpha}{4\alpha \sinh^2 \alpha}$$

Therefore

$$Q^* = \frac{1}{\beta p} + \frac{\alpha^3(\sinh 2\alpha - 2\alpha)}{12(\alpha \cosh \alpha - \sinh \alpha)^2} \tag{64}$$

For large α

$$\sinh \alpha \approx \cosh \alpha \approx \frac{e^\alpha}{2}$$

and

$$\lim_{\alpha\to\infty} Q^* = \frac{1}{\beta p} + \frac{\alpha}{6} \tag{65}$$

For small α, make a Taylor expansion in α for the numerator and denominator of Equation (64).

$$Q^* \approx \frac{1}{\beta p} + \frac{\alpha^3\left(2\alpha - 2\alpha + \frac{4}{3}\alpha^3\right)}{12\left(\alpha + \frac{\alpha^3}{2} - \alpha - \frac{\alpha^3}{6}\right)^2}$$

or

$$\lim_{\alpha\to 0} Q^* = \frac{1}{\beta p} + 1 \tag{66}$$

Since the transient term in each of these expressions is the reciprocal of the first moment, it is easy to see that it decays rapidly. Thus the above results show that for diffusion control, large α, the Q value is given by one-sixth the Thiele modulus (α) and for reaction control, small α, the Q value approaches unity. This demonstrates how diffusion can create a spread in the molecular weight distribution. The narrow distribution predicted for small α could be derived by ignoring diffusion; the resultant distribution is a Poisson distribution.

The molecular weight distribution for the solid core model may be derived easily using Equation (61). The reaction sites are all positioned at the surface of the sphere, and thus the distribution of sites $\theta(\eta)$ is a multiple of the dirac delta function.

$$\theta(\eta) = \delta(1) \tag{67}$$

Substitution of this into Equation (61) gives

$$Q^* = \frac{3}{\beta p} + 1 \tag{68}$$

A Poisson distribution is predicted regardless of the nature of diffusion.

MOLECULAR WEIGHT DISTRIBUTIONS FOR THE FLOW MODEL

The conservation equations for sites containing chains of i monomer units are, according to the flow model, as given by Equation (41), with the addition of terms to account for site convection:

$$\frac{\partial\theta_i}{\partial\tau} = \beta\alpha^2 c(\theta_{i-1} - \theta_i) - \frac{1}{\eta^2}\frac{\partial}{\partial\eta}(v\eta^2\theta_i)$$

$$\frac{\partial\theta_0}{\partial\tau} = \beta\alpha^2\theta_0 - \frac{1}{\eta^2}\frac{\partial}{\partial\eta}(v\eta^2\theta_0) \tag{69}$$

The manipulations which changed Equation (31) into the first-order partial differential equation (35) may be used here to convert Equations (69) to

$$\frac{\partial\theta_i}{\partial\tau} + v\frac{\partial\theta_i}{\partial\eta} = \beta\alpha^2 c(\theta_{i-1} - \theta_i) - \gamma\alpha^2 c\theta\theta_i$$

$$\frac{\partial\theta_0}{\partial\tau} + v\frac{\partial\theta_0}{\partial\eta} = -\beta\alpha^2 c\,\theta_0 - \gamma\alpha^2 c\theta\theta_0 \tag{70}$$

These equations may be solved along their characteristic curves, which are the particle paths described previously in Equation (36). They may be operated upon also to give equations for the moments analogous to Equations (43).

$$\left(\frac{\partial\lambda_0}{\partial\tau}\right)_\mu = -\gamma\alpha^2 c\theta^2$$

$$\left(\frac{\partial\lambda_1}{\partial\tau}\right)_\mu = -\gamma\alpha^2\theta c\lambda_1 + \beta\alpha^2 c\theta \tag{71}$$

$$\left(\frac{\partial\lambda_2}{\partial\tau}\right)_\mu = -\gamma\alpha^2\theta c\lambda_2 + \beta\alpha^2 c(2\lambda_1 + \theta)$$

These equations for the moments of the developing distribution were integrated numerically along the characteristic curves simultaneously with Equations (29), (34), and (35). The moments over the entire particle were evaluated at given times τ by integration of the local moments over the sphere according to Equation (45). For large α, the Q values for the entire particle were found to increase with polymer production p and decrease mildly after reaching a maximum as the value of polymer produced reached a value of about 100 times the catalyst volume.

The maximum Q value predicted by this model increases with α, as predicted by the stationary site models. A broader distribution (larger Q) is given by the flow model as shown in Figure 5. The maximum Q value appears to be independent of β.

For small α, the processes are reaction controlled and the flow model gives results identical to those of the polymeric core model because the sites are equally accessible to monomer. Thus a Poisson distribution is predicted for small α, and Q approaches unity.

Calculations were carried out for particles in batch reactors and continuous stirred-tank reactors. Results for Q values and the first three moments of the distributions were identical for both types of reactors in every case investigated. This useful result is the same as that found for the stationary site cases. This means that the molecular weight distribution depends only on the amount of polymer accumulated and the nature of the particle itself rather than the history of the particle.

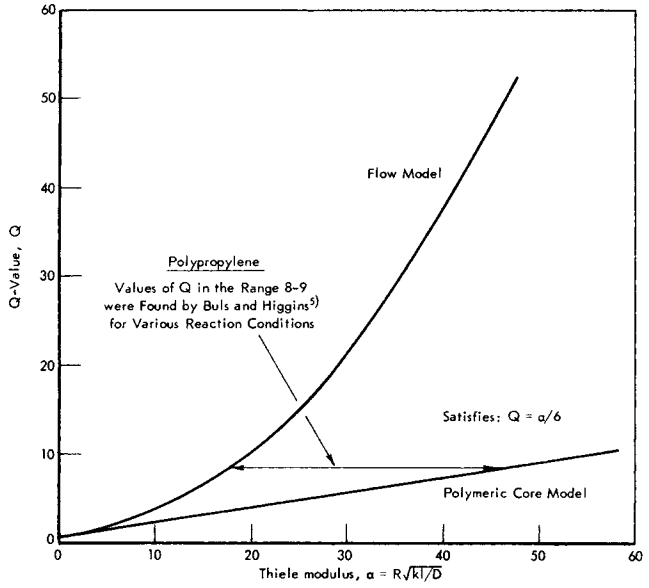

Fig. 5. Q value of the molecular weight distribution for polymer produced on a particle as a function of the Thiele modulus predicted by the expansion models.

SOME OBSERVATIONS ON α-OLEFIN POLYMERIZATIONS

Hock has shown that $TiCl_3$ catalyst, produced by the reduction of $TiCl_4$ with aluminum alkyls, consists of aggregates of particles in the size range, 100 to 1,000 Å (*8*). Buls and Higgins have confirmed this and have demonstrated, using electron microscopy, that polymer forms on these aggregates in such a way that the units retain their identity during polymerization (*5*). Furthermore, the aggregates of catalyst break up and become dispersed as small pieces in the polymer that is being produced from them.

We feel that the existence of the smaller units of a polymer globule is important in explaining the theory of replication presented by Berger and Grieveson (*3*) and Mackie et al. (*12*) for polyethylene. Polymer globules are observed to replicate the shape of the catalyst particles which produced them, with a magnification depending on yield which is often greater than 1,000 × (*18*). Catalysts which are shaped like needles, spheres, or pin cushions produce similar particles of polymer. This is illustrated by Mackie et al. (*12*).

Replication during a polymerization in which the particle grows in size by a factor of 1,000 or more would not be anticipated from consideration of the second law of thermodynamics or from rheology. Replication involves the transfer of information about catalyst shape through numerous events during the formation of a polymer globule. Magnification occurring at a given rate determines the local polymeric fluid acceleration and rate of strain. One would anticipate from rheological considerations that a constitutive equation between stress and rate of strain would apply during magnification which would result in stress being placed on interior and exterior particle surfaces acting to deform them.

Apparently the force relationships between the smaller units of a polymer globule dominate rheology and allow replications. Visualize a polymer globule at any time to be a multiply connected domain of arbitrary shape. The complementary domain may be disjoint; that is, the globule may be full of holes. Suppose the globule consists of infinitely small units of equal size which magnify at the same rate, retain their shape, and are constrained to keep their relative orientation to one another. Any curve in the domain grows at the same relative rate as the small units because it consists of segments which are chords within the units. A domain in which all curves contained in it grow at the same rate undergoes a magnification by definition.

Diffusion into the smaller polymer units and into the primary globule may be by different processes. We would anticipate polymeric diffusivities in the range 10^{-7} to 10^{-9} sq. cm./sec. for poly-α-olefins (*15*) to be important in the small units, and higher diffusivities to apply in the primary globule because of the existence of paths. Either or both could in theory be rate determining steps.

Different systems may exhibit different controlling mechanisms. Natta observed no effect of catalyst size on rate (*14*); yet Mackie et al. found that spheres and needles give polymers of different molecular weights in the same reactor (*12*). Constant rates (*3*) and declining rates (*6*) are observed.

Broad molecular weight distributions occur for cases of living polymer, and Buls and Higgins report Q values for isotactic polypropylene in the range 8 to 9 under batch reaction conditions of variable temperature, monomer concentration, and in the presence or absence of the termination agent, hydrogen (*5*). This might imply the existence of diffusion control and a value of the Thiele modulus between 10 and 50 if our models are applicable (see Figure 5). However, uncertainties in K_D, R, k, l, and D are great enough that these experiments cannot be used to discriminate between the complicated models described above and other models.

CONCLUSIONS

Four physical-mathematical models are presented for the expanding catalyst particles which are composed mainly of accumulating polymer. Polymerization rates and molecular weight distributions are predicted for each using a very simple kinetic model for the polymerization reaction.

1. In the base model, particle growth is ignored and catalyst sites are assumed to be dispersed evenly in a spherical matrix of polymer. For cases of reaction control or small Thiele modulus α, the polymerization rate is dependent on the local (site) rate constant and the distribution coefficient of monomer in polymer. A narrow molecular weight distribution is predicted.

For $\alpha = R\sqrt{kl/D} \ll 1$
Apparent rate constant, $k^* = V_p K_D kl$
Broadness of molecular weight distribution, $Q \cong 1$

For diffusion control, or large α, the rate dependence is distributed evenly between the rate constant and the diffusion parameter D/R^2. Solubility of monomer in polymer is always important. The molecular weight distribution broadens with increasing Thiele modulus.

For

$$\alpha \gg 1$$
$$k^* = 3V_p K_D \sqrt{klD/R^2}$$
$$Q = \alpha/6$$

2. In the solid core model, polymer is assumed to accumulate about a solid catalyst core, the surface of which supports the polymerization reaction. The reaction rate declines from its initial value to a final asymptotic value as the relative radius of the polymer coat η_S increases.

$$k^* = \frac{\dfrac{3V_p K_D D}{R^2}}{1 + \dfrac{3}{\alpha^2} - \dfrac{1}{\eta_S}}$$

For reaction control (small α) the apparent polymerization rate is dependent only on the reaction parameters and

is identical to the rate predicted by the base model. For diffusion control, the initial rate is the same as that for reaction control, but the asymptotic final rate is dependent only on the diffusion parameters.

For

$$\alpha \gg 1$$

$$k^* \longrightarrow 3V_p K_D D/R^2$$

Molecular weight distributions are in all cases narrow.

$$Q \approx 1$$

3. The first expansion model is a limiting case, the polymeric core model. Catalyst sites are assumed to be moving outward in a polymer matrix with negligible velocity. Thus this model is similar to the solid core model except that the core is polymeric and sites are dispersed evenly throughout it. The results for polymerization rates, using this model, are identical to those predicted using the solid core model. Molecular weight distributions are the same as those predicted using the base model.

4. The other expansion model is the flow model, in which sites are assumed to move outward unhindered by the expanding polymer matrix. This model and the previous one predict qualitatively similar behavior. For cases of diffusion control, the asymptotic rate predicted using the flow model is almost an order of magnitude larger than that predicted by the polymeric core model and a broader molecular weight distribution is predicted.

For

$$\alpha \gg 1$$

$$k^* \approx 30\, V_p K_D D/R^2 \text{ (asymptotic)}$$

$$Q \approx \alpha \text{ (asymptotic)}$$

For small α, or cases of reaction control, all models predict the same rate behavior and molecular weight distributions.

ACKNOWLEDGMENT

The concept of polymer globules expanding with catalysts dispersed within them was first put forth at this laboratory by V. W. Buls. Papers on this subject by V. W. Buls and T. L. Higgins have been published in *The Journal of Polymer Science*. See reference (5).

NOTATION

c = dimensionless monomer concentration in polymer
c_S = dimensionless monomer concentration at surface of polymer globule
$c^*(\tau)$ = dimensionless monomer concentration at boundary of catalyst core
D = diffusivity of monomer in polymer
$f(\alpha)$ = dimensionless apparent rate constant
G = saturation ratio, $3V_p K_D$
k = local polymerization rate constant (second order), volume catalyst/(time)(site)
k^* = apparent polymerization rate constant (first order), 1/(time)
K_D = distribution coefficient of monomer in polymer, conc. in polymer/(conc. in solution)
l = site concentration, sites/volume
l_i = concentration of sites containing polymer chains with i monomer units, sites/volume
l_A = reference site concentration, sites/volume
M = monomer concentration in polymer
M_N = number average molecular weight
M_W = weight average molecular weight
m = molecular weight of monomer
p = dimensionless moles of polymer per unit volume of catalyst (referred to a reference monomer concentration in the polymer)
Q = local Q value, M_W/M_N or $\lambda_0\lambda_2/\lambda_1^2$
Q^* = Q value for the entire particle
R = initial radius of particle, length
r = radial variable, length
s = characteristic-independent variable of the partial differential equation, in this case, $s = \tau$
t = time variable
T = characteristic time of a process
u = velocity of sites or forming polymer, length/time
v = dimensionless velocity, uR/D
V_p = volume of particles per unit volume of solution

Greek Letters

α = Thiele modulus, $R\sqrt{kl/D}$
β = ratio of reference monomer concentration to reference site concentration
γ = dimensionless specific volume of polymer (referred to reference monomer concentration in polymer), (reference monomer conc) (vol.)/(mol. polymerized monomer)
$\delta(\eta)$ = dirac delta function
η = dimensionless radial variable, r/R
η_S = dimensionless radius of sphere (referred to original radius)
ρ = molar density polymer, moles polymerized monomer/volume
μ = characteristic-independent variable of the partial differential equation
λ_n = dimensionless local n^{th} moment of distribution, $\sum_{i=0}^{\infty} i^n \theta_i$
λ_n^* = dimensionless n^{th} moment for entire particle
ϕ = solution to a differential equation
τ = dimensionless time, tD/R^2
θ = dimensionless site concentration, l/l_A
θ_i = dimensionless concentration of sites containing polymer chains with i monomer units, l_i/l_A

LITERATURE CITED

1. Aris, Rutherford, "Vectors, Tensors, and the Basic Equations of Fluid Mechanics," p. 76, Prentice-Hall, Englewood Cliffs, N. J. (1962).
2. Begley, J. W., *J. Polymer Sci.*, Part A-1, **4**, 319 (1966).
3. Berger, M. N., and B. M. Grieveson, *Makromol. Chem.*, **83**, 80 (1965).
4. Billmeyer, F. W., Jr., "Textbook of Polymer Science," pp. 56, 66, Interscience, New York (1962).
5. Buls, V. W., and T. L. Higgins, *J. Polymer Sci.*, **8**, 1025, 1037 (1970).
6. Count, A. D., *ibid.*, **C4**, 49 (1964).
7. Grieveson, B. M., *Makromol. Chem.*, **84**, 93 (1965).
8. Hock, C. W., *J. Polymer Sci.*, Part A-1, **4**, 3055 (1966).
9. Lapidus, Leon, "Digital Computations for Chemical Engineers," p. 88, McGraw-Hill, New York (1962).
10. Lehman, G., and A. Gumboldt, *Makromol. Chem.*, **70**, 23 (1964).
11. Lipman, R. D. A., and R. G. W. Norrish, *Proc. Roy. Soc. (London)*, **A275**, 310 (1963).
12. Mackie, P., M. N. Berger, B. M. Grieveson, and D. Lawson, *Polymer Letters*, **5**, 493 (1967).
13. Mark, H. F., *Amer. Sci.*, **55**, 265 (1967).
14. Natta, G., and I. Pasquon, *Advan. Catalysis*, **11**, 1 (1959).
15. Raff, R. A. V., and K. W. Doak, Eds., "Crystalline Olefin Polymers, Part II," Interscience, New York (1964).
16. Seinfeld, J. H., California Inst. Tech., private communication (Sept. 24, 1968).
17. Wilson, T. P., and G. F. Hurley, *J. Polymer Sci.*, **C1**, 281 (1963).
18. ———, *Stauffer Chem. Co., Tech. Bull.*, Weston, Mich. (1962).

Manuscript received February 5, 1969; revision received November 3, 1969; paper accepted November 6, 1969.